

The Granular Chloride Channel CIC-3 Is Permissive for Insulin Secretion

Ludmila V. Deriy,¹ Erwin A. Gomez,¹ David A. Jacobson,² XueQing Wang,¹ Jessika A. Hopson,¹ Xiang Y. Liu,³ Guangping Zhang,¹ Vytautas P. Bindokas,¹ Louis H. Philipson,² and Deborah J. Nelson^{1,*}

¹Department of Neurobiology, Pharmacology, and Physiology

²Department of Medicine

³Department of Surgery

The University of Chicago, Chicago, IL 60637, USA

*Correspondence: nelson@uchicago.edu

DOI 10.1016/j.cmet.2009.08.012

SUMMARY

Insulin secretion from pancreatic β cells is dependent on maturation and acidification of the secretory granule, processes necessary for prohormone convertase cleavage of proinsulin. Previous studies in isolated β cells revealed that acidification may be dependent on the granule membrane chloride channel CIC-3, in a step permissive for a regulated secretory response. In this study, immuno-EM of β cells revealed colocalization of CIC-3 and insulin on secretory granules. *Clcn3*^{-/-} mice as well as isolated islets demonstrate impaired insulin secretion; *Clcn3*^{-/-} β cells are defective in regulated insulin exocytosis and granular acidification. Increased amounts of proinsulin were found in the majority of secretory granules in the *Clcn3*^{-/-} mice, while in *Clcn3*^{+/+} cells, proinsulin was confined to the immature secretory granules. These results demonstrate that in pancreatic β cells, chloride channels, specifically CIC-3, are localized on insulin granules and play a role in insulin processing as well as insulin secretion through regulation of granular acidification.

INTRODUCTION

Considerable progress has been made in determining many features of secretagogue-regulated insulin secretion, particularly the role of vesicle-associated ion channels in granule release (Rorsman and Renström, 2003). However, we are still at an early stage in defining the molecular mechanisms involved in exocytosis of the insulin granule and the important role of granule membrane ion channels in granule release. Vesicular ion channels may play several roles in secretion in addition to facilitating a specific requirement for vesicle acidification, as in the case of insulin secretion. The chloride channel CIC-3, originally identified in swelling of insulin-secreting HIT cells (Kinard et al., 2001), is expressed in the membrane of insulin-containing granules. Previous functional studies in isolated β cells using channel-specific inhibitory antibodies to elucidate CIC-3 functional expression showed that activation of CIC-3 is permissive for insulin secretion (Barg et al., 2001).

This is due, at least in part, to the promotion of insulin granule acidification; various strategies to abolish acidification disrupt secretion in a similar manner. We have extended the earlier findings of Barg et al. (Barg et al., 2001) on the functional expression of CIC-3 in insulin granules to the CIC-3 knockout mouse.

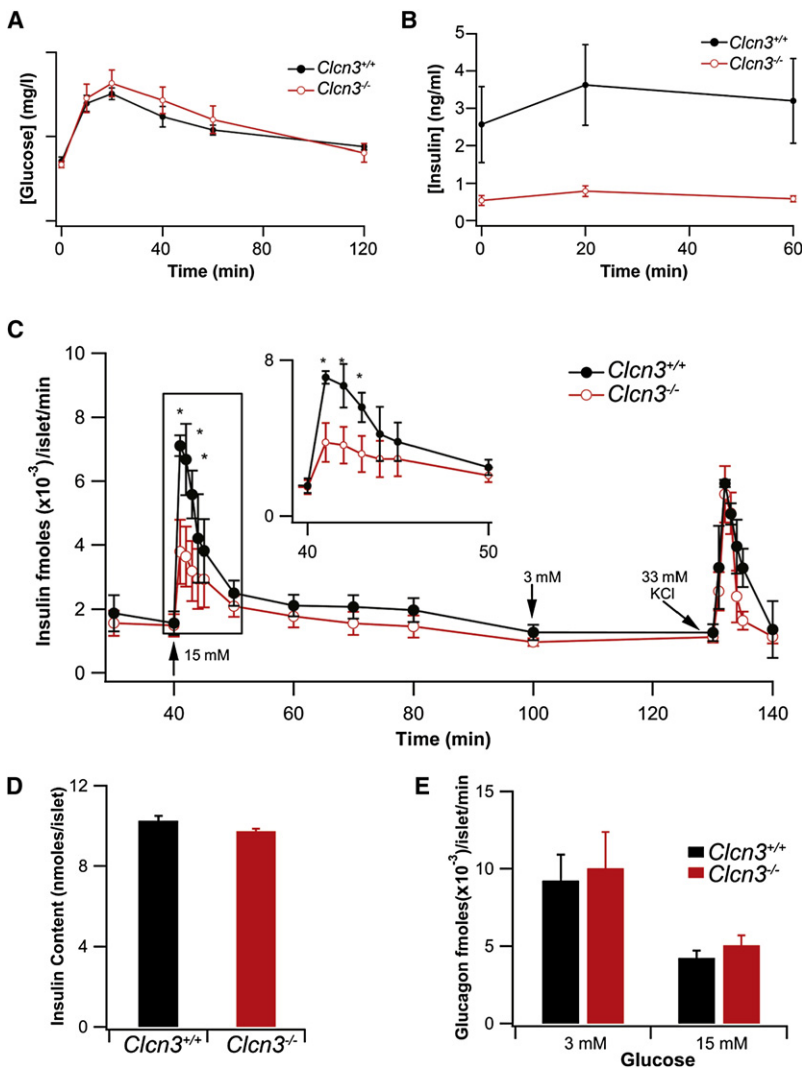
A recent paper by Maritzen and colleagues (Maritzen et al., 2008) concluded that CIC-3 is localized not in large dense-core vesicles (LDCVs), but rather in smaller, noninsulin-containing vesicles, in contrast to our earlier studies (Barg et al., 2001). The Maritzen et al. studies relied heavily on subcellular fractionation using homogenates of the insulin-secreting cell line INS-1 and detected little CIC-3 in the LDCV fraction. Our current study, using primary β cells, clearly shows colocalization of insulin and CIC-3 in LDCVs using high-resolution immuno-EM, a method more suitable for examining channel localization. In addition, we present physiological evidence demonstrating an indisputable effect of CIC-3 expression on granule pH and insulin processing in primary β cells.

We have obtained compelling data, the analysis of which suggests that CIC-3 is gated by CaMKII in various systems (Huang et al., 2001; Mitchell et al., 2008; Robinson et al., 2004; Wang et al., 2006). Given that CaMKII is implicated in insulin secretion (Easom, 1999; Easom et al., 1997; Gromada et al., 1999; Krueger et al., 1997) and the previously published findings that CIC-3 contributes to insulin granule acidification and, therefore, granule maturation, we carried out experiments on *Clcn3*^{-/-} mice to determine whether the chloride channel played a significant role in the process of pancreatic β cell granule maturation, mobilization, and finally release.

RESULTS

Impaired Insulin Secretion in Transgenic *Clcn3*^{-/-} Mice

Given that CIC-3 Cl⁻ channels localize to the β cell granule membrane and contribute to granule acidification and mobilization (Barg et al., 2001), we anticipated that *Clcn3*^{-/-} mice might manifest defective insulin secretion. Data in Figure 1 indicate that null mice exhibit a relatively normal glucose tolerance as compared to wild-type (WT) littermates (Figure 1A). Glucose tolerance responses between subsets of *Clcn3*^{-/-} animals showed a high degree of variability. This could be due to an increase in insulin sensitivity in peripheral tissues and/or differences in post-insulin receptor signaling in muscle and fat in



subsets of *Clcn3*^{-/-} animals, indicative of a secondary compensation resulting from the global loss of CIC-3 channels. In contrast, serum insulin levels were significantly reduced in the *Clcn3*^{-/-} animals over the *Clcn3*^{+/+} littermate controls (Figure 1B), consistent with a β cell secretory defect.

Having observed a significant difference in serum insulin levels between the CIC-3 WT and null mice, we examined whether a similar secretory impairment could be observed in islets isolated from *Clcn3*^{-/-} animals. Perfusion assays of isolated islets revealed that first-phase glucose-stimulated insulin release was significantly attenuated in the *Clcn3*^{-/-} islets as compared to islets from *Clcn3*^{+/+} animals (Figure 1C). Insulin release in response to maximal K⁺-induced depolarization, total islet insulin content, and glucagon release in response to glucose did not vary between the two genotypes (Figures 1C–1E). It is intriguing to note that insulin secretion to glucose is impaired, but not to high K⁺, as both stimuli produce cellular depolarization and stimulate insulin release by a mechanism upstream of acidification. This apparent discrepancy suggests that CIC-3 may also play a role in the pathway between glucose metabolism and cellular depolarization.

Figure 1. Serum Glucose and Insulin Levels in *Clcn3*^{-/-} Mice Compared to Wild-Type (*Clcn3*^{+/+}) Littermate Controls, Blunted First-Phase Insulin Secretion in *Clcn3*^{-/-} Islets

(A) Blood glucose levels were measured in whole blood following glucose challenge; $n_{Clcn3^{+/+}} = 6$, $n_{Clcn3^{-/-}} = 10$. Data are plotted as the mean \pm SEM. (B) Insulin concentration was measured in sera of *Clcn3*^{-/-} ($n = 7$) and *Clcn3*^{+/+} ($n = 3$) mice by ELISA; $n_{Clcn3^{+/+}} = 6$, $n_{Clcn3^{-/-}} = 10$. Data are plotted as the mean \pm SEM. Note timescale differences in (A) and (B). (C) Insulin release from isolated perifused islets from WT (closed black circles) and KO (open red circles) mice before and after elevating glucose from 3 mM to 15 mM and back to 3 mM. Data are presented in fmoles $\times 10^{-3}$ of insulin/islet/min as means \pm SEM ($n = 3$). Asterisks mark significance at the $p < 0.05$ level. (D) Total insulin content in the lysed islets, measured by ELISA as in (B) and (C). Data are presented in nanomoles of insulin/islet. Data are mean \pm SEM. (E) Glucagon concentration was determined in the same fractions by ELISA. Data are presented in fmoles $\times 10^{-3}$ of glucagon/islet/min as means \pm SEM ($n = 3$).

Reduced Secretion in β Cells from *Clcn3*^{-/-} Mice

The characteristic pattern of insulin secretion in response to glucose seen at the whole-animal or organ level is reflected electrophysiologically in isolated β cells by transient increases in membrane capacitance when cells are stimulated with square-wave depolarizing pulses that open plasma membrane L-type voltage-dependent Ca²⁺ channels (Ammälä et al., 1993). In order to confirm the role of CIC-3 in the regulation of depolarization-induced granular release, we carried out studies on β cells isolated from both *Clcn3*^{+/+} and *Clcn3*^{-/-} mice. Data in Figures 2A and 2B demonstrate

that a fast-phase (ready releasable pool [RRP]) of secretion, as measured by a rapid increase in membrane capacitance elicited by a single depolarizing voltage pulse, is reduced in *Clcn3*^{-/-} cells. Refilling of the RRP in *Clcn3*^{-/-} mice is inhibited, as shown by a decreased membrane capacitance in response to the first depolarization in a train of depolarizing stimuli in a slow phase (Figures 2A and 2B). The rate of capacitance increase in β cells isolated from *Clcn3*^{-/-} mice was lower than in *Clcn3*^{+/+} mice, with the average rate of capacitance change (ΔC_m in pF/s) of $9.5 \times 10^{-3} \pm 1.5 \times 10^{-3}$ for *Clcn3*^{+/+} and $-4.3 \times 10^{-3} \pm 3.1 \times 10^{-3}$ for *Clcn3*^{-/-} (Figure S1). The decrease in depolarization-induced secretion seen in the *Clcn3*^{-/-} β cells was not due to a decrease in the density of voltage-dependent channels. The peak and steady-state Ca²⁺ channel current density in response to step depolarizations from a holding potential from -70 to 0 mV was not significantly different between the *Clcn3*^{+/+} and *Clcn3*^{-/-} cells (Figures 2C and 2D).

Interestingly, we observed endocytosis following a single depolarization in a train (Figure S2). During the 500 ms interval between pulses, capacitance rose and then fell prior to the succeeding pulse, often leading to a negligible net increase between

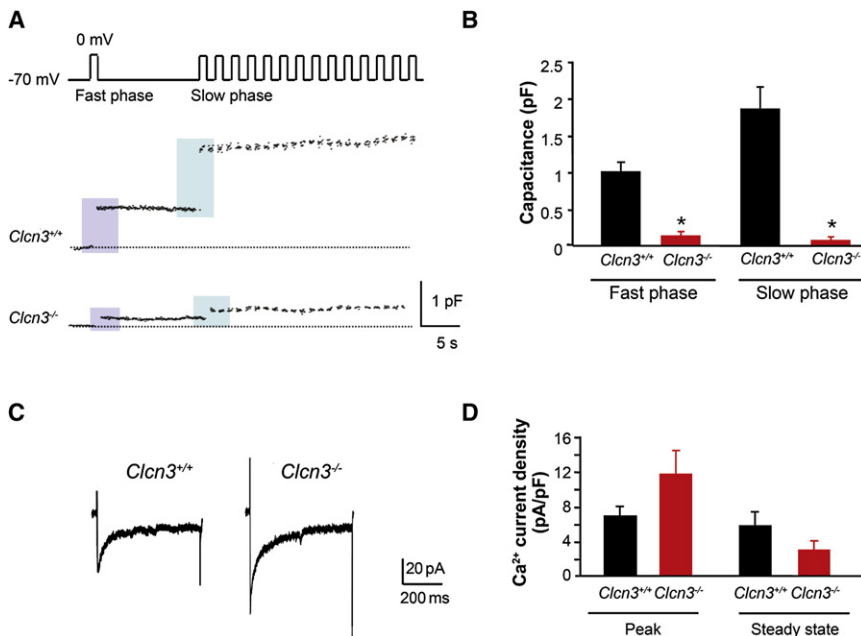


Figure 2. Reduction in Depolarization-Induced Exocytosis in Pancreatic β Cells Isolated from *Clcn3*^{-/-} Mice Compared to *Clcn3*^{+/+}

(A) Perforated patch recordings from representative pancreatic β cells showing increases in cell membrane capacitance (ΔC_m) evoked by voltage-clamp depolarizations from -70 to 0 mV (500 ms, 1 Hz).

(B) Histograms showing average changes in capacitance during fast and slow phase of secretion. Fast-phase secretion (from a docked RRP) was triggered by a single pulse from -70 to 0 mV (500 ms) 10 s before the train was applied to the cells to elicit mobilization of granules from a reserve pool of granules (slow phase). Data are mean ± SEM of four experiments for each cell type. *p < 0.05.

(C) Representative whole-cell Ca²⁺ currents from perforated patch capacitance experiments as in (A). Currents were elicited by 500 ms voltage-clamp depolarizations from -70 to 0 mV.

(D) Summary of average changes in peak and steady-state Ca²⁺ current in *Clcn3*^{+/+} and *Clcn3*^{-/-} cells. Neither average peak nor steady-state currents were significantly different from one another. Data are mean ± SEM of four experiments for each cell type.

pulses. To our knowledge, this has not been observed in whole-cell capacitance studies of β cells to date. We observed this behavior in approximately 50% of the *Clcn3*^{+/+} and none of the *Clcn3*^{-/-} cells examined.

CIC-3 Localization in Insulin Granules of Pancreatic β Cells

Electron microscopy on thin sections of pancreatic islets clearly demonstrates localization of CIC-3 on insulin granules (Figure 3A). No staining with preimmune IgG was observed (data not shown). Control experiments where anti-CIC-3 antibody was depleted with 10-fold molar concentration of soluble insulin prior to staining confirmed that the presence of CIC-3 on insulin granules is not due to nonspecific recognition of insulin by anti-CIC-3 antibody or nonspecific interaction of anti-CIC-3 and anti-insulin antibodies (Figure S3).

Proinsulin Subcellular Localization

The foregoing observations demonstrating that insulin release in the *Clcn3*^{-/-} mouse is compromised at the whole-animal, isolated islet, and single β cell levels suggested that this may be due to either a decrease in β cell insulin granule content or, alternatively, impairment in insulin processing within the granules (Rouillé et al., 1995).

The prohormone convertase (PC) insulin processing enzyme has an acidic pH optimum. Therefore, if granules from *Clcn3*^{-/-} β cells are not acidified, we would expect a rise in proinsulin and a fall in insulin levels similar to that seen in granules in β cells isolated from PC 1/3 null (*pc1/3*^{-/-}) mice (Zhu et al., 2002). We probed this possibility at the electron microscopic level. Results in Figure 3B indicate that granules from *Clcn3*^{-/-} mice are less dense than WT, a characteristic indicator of impaired granule processing from proinsulin to insulin (Furuta et al., 1998;

Zhu et al., 2002). Granule number did not significantly vary between genotypes (data not shown). An examination of *Clcn3*^{-/-} β cell granules showing increased levels of proinsulin as compared to granules from WT β cells can be seen in Figure 3C. Proinsulin labeling was carried out on thin sections of pancreatic β cells using the proinsulin monoclonal antibody GS-9A8 and examined by immuno-EM. In contrast to WT β cells, where proinsulin staining was confined to the Golgi and nascent (maturing) secretory granules, proinsulin staining in the *Clcn3*^{-/-} β cells was observed in the majority of the secretory granules, both maturing and at endpoint (plasmalemmal location).

Granular Acidification Defect in *Clcn3*^{-/-} β Cells

It has been shown previously that interference with granular acidification reduces exocytosis in β cells (Barg et al., 2001). In order to compare granular acidification in *Clcn3*^{-/-} and *Clcn3*^{+/+} cells, we carried out live-cell microscopy on isolated β cells using the ratiometric, acidotropic dye LysoSensor Yellow/Blue DND-160 that has recently been applied to β cell granules by Stiernet et al. (Stiernet et al., 2006). If granule acidification is dependent on CIC-3 activity, then the granule population in β cells isolated from *Clcn3*^{-/-} mice should be relatively alkalotic as compared to similar populations in *Clcn3*^{+/+} β cells. Given that the acid-sensitive dye accumulates in all acidic organelles, including lysosomes, we restricted our confocal imaging and analysis to regions of the cells likely to represent a high density of subplasmalemmal granules. In these experiments, we used a dual-emission protocol where cells excited with 405 nm showed pH-sensitive emission at 510 nm and pH-insensitive emission at 485 nm (Figure 4). The corresponding pH values for 510/485 nm ratios were obtained from an in situ calibration curve (Figure 4C) by interpolation. The curve was constructed using a cocktail of ionophores to clamp the intracellular

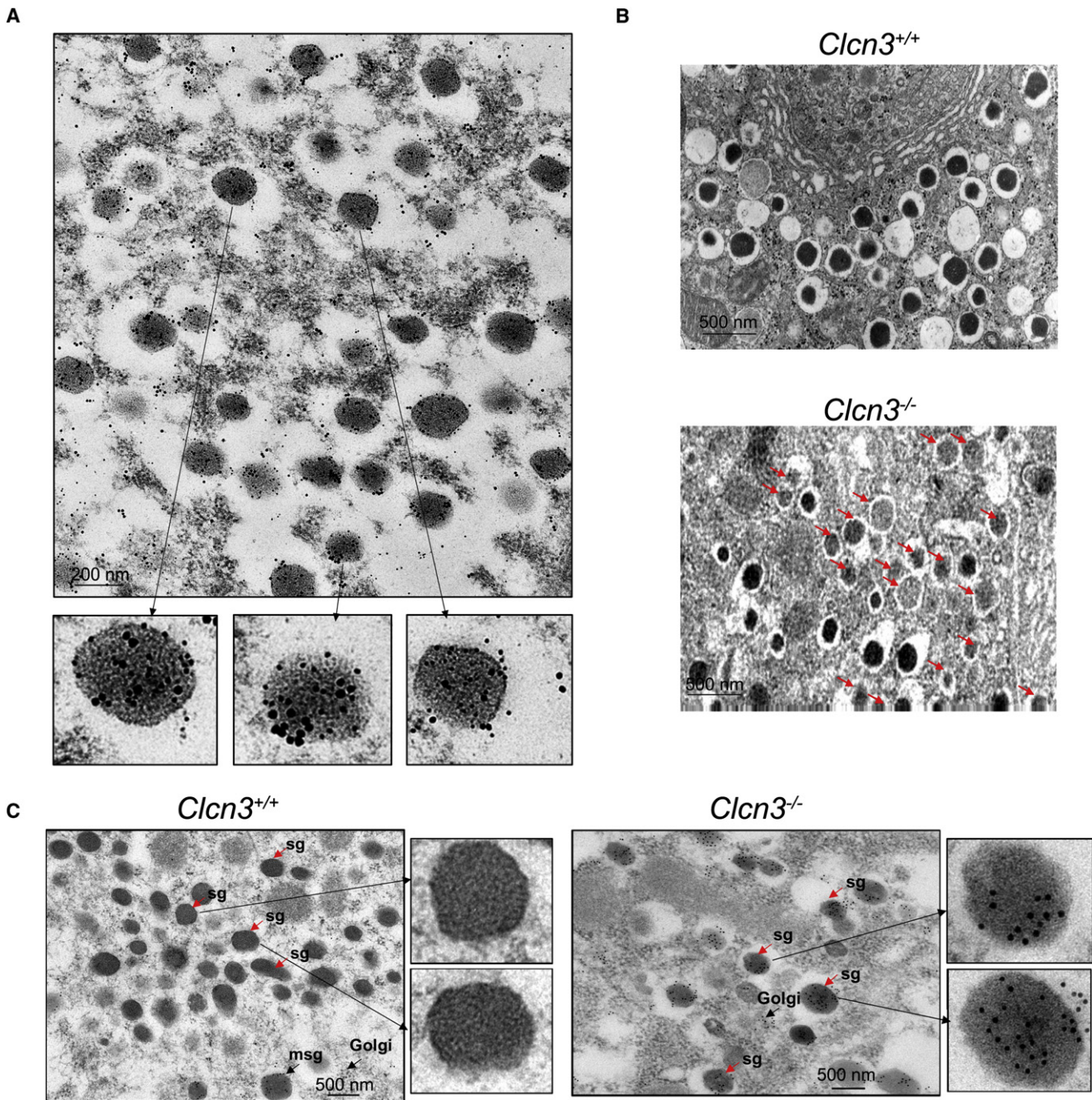


Figure 3. Electron Microscopic Localization of CIC-3 on Insulin Granules and Characterization of Secretory Granules in Thin Sections of β Cells from $Clcn3^{+/+}$ and $Clcn3^{-/-}$ Mice

(A) Immunogold staining shows insulin (10 nm particles) and CIC-3 (15 nm particles) colocalized in secretory granules of β cells.

(B) Comparison of $Clcn3^{+/+}$ and $Clcn3^{-/-}$ cells reveals abundant pale, immature-appearing secretory granules in the knockout cells (marked by arrows).

(C) Localization of proinsulin in thin sections of pancreatic β cells from $Clcn3^{+/+}$ and $Clcn3^{-/-}$ mice. In $Clcn3^{+/+}$ mice, proinsulin staining is observed only in the nascent (maturing) secretory granules (msg). Mature secretory granules (sg) appear free of labeling. In the β cells from the $Clcn3^{-/-}$ mice, proinsulin labeling is found regardless of the state of maturity.

pH at a known value (smooth curve through the data points in Figure 4C). Data show that WT cells had a significantly higher acidification index than did the $Clcn3^{-/-}$ cells (Figures 4A and 4B). Their 510/485 nm ratio was 1.5 ± 0.03 , corresponding to a pH of 4.79 in subplasmalemmal granules. In situ calibration

of the dye in double-excitation experiments (excitation at 340 and 380 nm, emission at 535 nm) also showed that WT cells exhibited a granular pH of 4.8 ± 0.1 ($n = 112$) (data not shown). The pH sensitivity of the dye ($pK_a = 4.2$) precluded accurate in situ dye calibration at pH values greater than 5.2 in the fluorescence

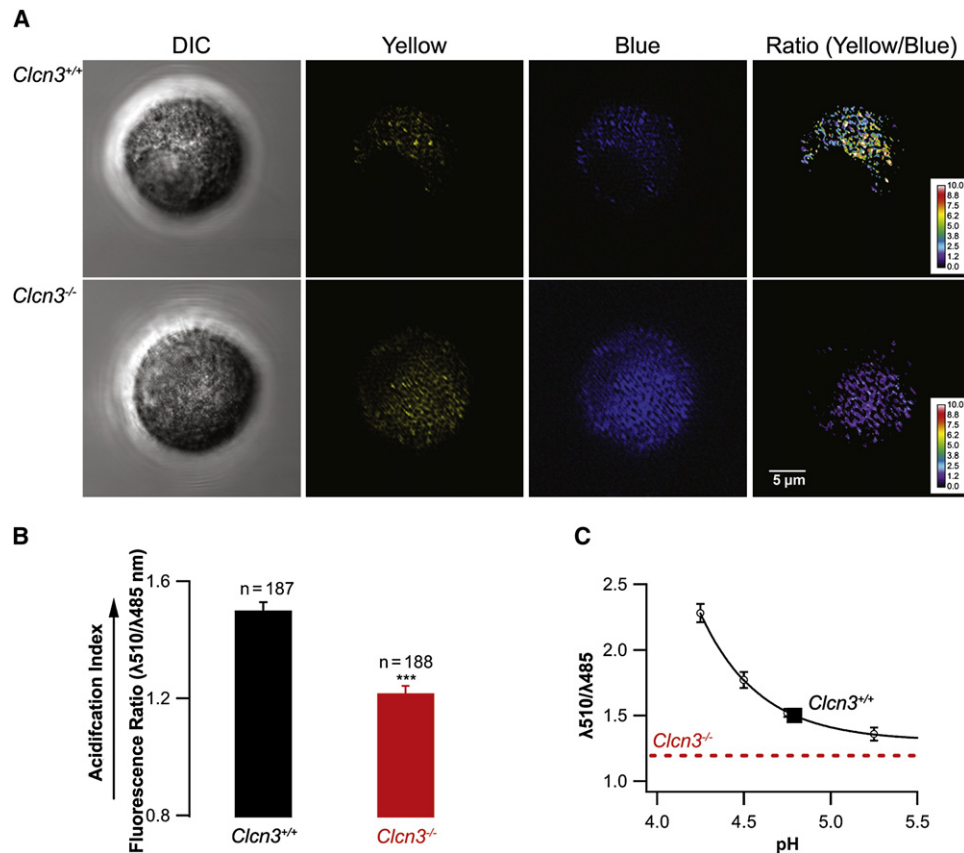


Figure 4. Granule Acidification in β Cells Isolated from *Clcn3*^{+/+} and *Clcn3*^{-/-} Mice

(A) Pancreatic β cells were loaded with the pH-sensitive, ratiometric dye LysoSensor Yellow/Blue DND-160 and visualized with confocal microscopy. Dye-filled vesicles were imaged at the polar focal plane (close to the cell surface to maximize the analysis of secretory granules). The ratio of yellow (pH-sensitive) to blue (pH-insensitive) emission was used to determine organellar pH.

(B) Results were analyzed using ImageJ software and presented as mean 510/485 nm fluorescence ratios \pm standard errors.

(C) In situ calibration curve was used to determine pH values corresponding to 510/485 nm ratios obtained experimentally. The dotted line corresponds to the experimentally obtained fluorescence ratio in *Clcn3*^{-/-} cells. The ratio was significantly less than that of the *Clcn3*^{+/+} cells and corresponded to the asymptotic part of the pH calibration curve, making an estimate of the corresponding pH ambiguous (see text). Data are mean \pm SEM.

ratio range of the *Clcn3*^{-/-} cells. Thus, the pH of the alkalotic *Clcn3*^{-/-} granules can be estimated as at least one full pH unit greater than that of CIC-3-expressing cells.

DISCUSSION

Results described in this study establish that the Cl⁻ channel CIC-3 is critical in the control of insulin release at the whole-animal, isolated islet, and single β cell levels. Our data provide evidence that CIC-3 expressed on secretory granule membranes is involved in the maintenance of a low intragranular pH (pH_g), a phenomenon increasingly recognized as important to secretion. Cl⁻ entry across the granule membrane is thought to be required to shunt H⁺ influx via the V-ATPase, thus preventing the buildup of a large transgranular membrane potential.

Until recently, anion channels have received relatively little attention, as compared to their cation channel cousins, in the context of regulated insulin release. The complexity of Cl⁻ channels became apparent with the cloning of an evolutionarily conserved family of Cl⁻ channels (CICs), as well as the discovery

of other channel families that principally carry Cl⁻ (e.g., CFTR, Ca²⁺-activated Cl⁻ channels) (Jentsch et al., 2002). CIC-3 is a member of the former category and is widely distributed in mammalian tissues. It can assume either a plasma membrane or intracellular membrane localization and has been proposed as the channel mediating acidification in endosomes (Hara-Chikuma et al., 2005; Mitchell et al., 2008). Mice lacking CIC-3 exhibit a variety of defects, most prominently postnatal degeneration of the hippocampus and photoreceptors (Dickerson et al., 2002; Stobrawa et al., 2001; Yoshikawa et al., 2002). CIC-3 is present on synaptic vesicles and may play a role in glutamatergic neurotransmitter release (Stobrawa et al., 2001). Indeed, we have recently shown that CIC-3 shapes synaptic currents in developing hippocampal neurons, in part, by studying *Clcn3*^{-/-} mice (Wang et al., 2006).

To understand the molecular basis of secretion, it is important to have assays that analyze single vesicle (granule) events and to be able to manipulate individual molecules thought to be important in the process. Capacitance measurements of cell surface area have been utilized in many systems, including β cells (Bokvist

et al., 2000; Göpel et al., 2004; Kanno et al., 2004; Rorsman and Renström, 2003), to investigate pools of vesicles and their role in secretion. These studies have shown that, in β cells, the transient first phase of insulin secretion is mediated by a docked pool of vesicles termed the RRP, while the sustained second phase is due to mobilization of vesicles from a reserve pool into the RRP. Mobilization involves “priming” of the vesicles, a stage requiring ATP hydrolysis, but whether there are single or multiple ATP-requiring processes is unclear. Exocytosis itself is almost certainly mediated by a SNARE mechanism that promotes vesicle fusion in many regulated secretory systems (Eliasson et al., 2008).

In the capacitance experiments of Barg et al. (Barg et al., 2001) conducted on isolated murine β cells, intrapipette (intracellular) application of a functional inhibitory antibody directed against a peptide in the cytoplasmic C-terminal domain of CIC-3 significantly reduced the late slow component of exocytosis corresponding to the filling of the RRP of granules from the reserve pool (Barg et al., 2001). A comparative analysis of the size of the RRP under similar conditions was not determined in their studies. In our experiments, both fast phase (triggered by the first depolarization) and the later component of exocytosis, slow phase triggered with a train of depolarizations following a refilling period, were significantly inhibited in cells isolated from *Clcn3*^{-/-} mice. In contrast to data using CIC-3 inhibitory antibodies (Barg et al., 2001), our data using *Clcn3*^{-/-} β cells are consistent with a model in which CIC-3 plays a role in determining both the size or release competency of the granular RRP as well as the rate of replenishment of the granular RRP from the reserve pool.

Granule Acidification Mechanism and Potential Functions

It has been known for some time that the pH_g of insulin granules is acidic ($pH_g \approx 5-6$, with a decrease during granule maturation) (Abrahamsson and Gylfe, 1980; Hutton, 1982; Orci et al., 1986; Pace and Sachs, 1982). Recent studies in mouse islets have shown that glucose causes an acute decrease in pH_g that is dependent on the metabolism of glucose and cytoplasmic Cl^- (Stiernet et al., 2006). These results suggest that there is a pathway from glucose metabolism that augments acidification, possibly by increasing Cl^- movement into the granule. One important function of an acidified granular lumen is to promote the conversion of proinsulin to insulin by PCs (PC1, PC2, and PC3) that have an acidic pH optimum (Rouillé et al., 1995). Other granule constituents that are substrates for PCs (like islet amyloid polypeptide [IAPP]) may also be dependent on acidification. The slow phase of glutamate release from synaptosomes (Zoccarato et al., 1999) shows pH dependence similar to that we have observed for β cell granules, suggesting that the model developed in β cells may be universal for all Ca^{2+} -regulated secretion. Moreover, our data suggest that low pH_g may be required not only for the priming of the granules, but also for the maintenance of the granules in a releasable state. These observations are in good agreement with those made in pituitary melanotrophs (Thomas et al., 1993), glucagon-releasing pancreatic α cells (Høy et al., 2000), and chromaffin granules (Camacho et al., 2006; Pothos et al., 2002). Consequently, it may well be that development of a low pH_g is required for other aspects of granule physiology that impact the priming step.

Although it is still unclear whether the regulation of granule acidification can be directly connected with the development of human type 2 diabetes and the CIC-3 gene itself has not been so far implicated in the pathogenesis of type 2 diabetes, this study suggests that a CIC-3-mediated mechanism leading to impaired granule acidification and proinsulin processing could contribute to diabetes, especially in the context of insulin resistance.

EXPERIMENTAL PROCEDURES

Animals

All experiments on mice were performed in accordance with the University of Chicago and national guidelines and regulations and were approved by the University of Chicago Institutional Animal Care and Use Committee. *Clcn3*^{-/-} mice and WT control littermates were bred at the Animal Core Facility of the University of Chicago and genotyped as described previously (Dickerson et al., 2002).

Glucose Homeostasis

Blood glucose and insulin concentrations were measured in 8-week-old male *Clcn3*^{-/-} and littermate controls after a 4 hr fast, then at the indicated times following intraperitoneal injection of glucose (2 g/kg) using a Freestyle blood glucose monitor (Therasense, Inc.; Alameda, CA) and mouse ultrasensitive ELISA (Alpco Diagnostics; Salem, NH).

Islet Perfusion Assay

Fifty islets per mouse were loaded into columns and perfused with modified Krebs-Ringer buffer containing 0.5% BSA and the indicated concentrations of glucose or KCl using a temperature-controlled automated perfusion system (Biorep Technologies, Inc.; Miami, FL). Outflow was collected, and hormone concentrations were measured by mouse insulin (Alpco Diagnostics) and glucagon ELISA (Phoenix Pharmaceuticals, Inc.; Burlingame, CA). To determine total insulin content, islets were lysed by passing 2% Triton X-100 through the column. See Supplemental Data for detailed procedure.

Electrophysiology

Procedure for perforated patch capacitance recordings may be found in the Supplemental Data.

Electron Microscopy

Isolated islets were prepared for electron microscopy as described previously (Barg et al., 2001). Fixed sections were treated as indicated with anti-insulin polyclonal antibody raised in guinea pig (Millipore; Bedford, MA), custom-made anti-CIC-3 polyclonal antibody raised in rabbit (Huang et al., 2001), or anti-proinsulin monoclonal antibody GS-9A8, a generous gift of Dr. O. Madsen (BCBC Antibody Core Unit, Novo Nordisk; Malov, Denmark). Secondary antibodies conjugated to gold particles (Ted Pella, Inc.; Redding, CA) were used for visualization.

Fluorescence Microscopy

Isolated β cells were loaded with LysoSensor Yellow/Blue DND-160 (Molecular Probes; Eugene, OR) and visualized using a Leica SP2 confocal microscope using 63 \times NA 1.5 oil objective. The preparations were excited at 405 nm, and emission was recorded at the range of 485 \pm 20 nm for blue (pH-insensitive) and 510 \pm 20 nm for yellow (pH-sensitive) fluorescence. Images were taken at the polar focal plane, ROIs were drawn around fluorescent spots representing docked vesicles, and intensities were measured at each emission band. Results were analyzed using ImageJ software and presented as mean 510/485 fluorescence ratios \pm SEM. The pH values of the measured ratios were determined by interpolation using the in situ calibration curve.

In Situ pH Calibration Curve

In situ pH calibration curve was performed as described in the Supplemental Data.

Statistical Analyses

Statistical comparisons were performed using Student's *t* test. Unless otherwise stated, all data are expressed as a mean \pm SEM with the number of experiments in parentheses.

SUPPLEMENTAL DATA

Supplemental Data include Supplemental Experimental Procedures, Supplemental References, and three figures and can be found online at [http://www.cell.com/cell-metabolism/supplemental/S1550-4131\(09\)00262-9](http://www.cell.com/cell-metabolism/supplemental/S1550-4131(09)00262-9).

ACKNOWLEDGMENTS

This work was supported in part by the NIH (R01 GM36823 and R01 DK080364 to D.J.N.). L.H.P. is partially supported by the NIH (R01 DK48494 and R01 DK063493) and by The University of Chicago Diabetes Research and Training Center (P60 DK20595). The authors thank Ole D. Madsen (Hagedorn Research Institute, Denmark) for the gift of monoclonal antibody GS-9A8 and Yimei Chen at the University of Chicago Electron Microscopy Core Facility for her help with immuno-EM. The authors also wish to thank D.F. Steiner, C.J. Rhodes, and H.C. Palfrey (The University of Chicago) for many helpful discussions during the course of this investigation.

Received: January 27, 2009

Revised: July 6, 2009

Accepted: August 18, 2009

Published: October 6, 2009

REFERENCES

- Abrahamsson, H., and Gylfe, E. (1980). Demonstration of a proton gradient across the insulin granule membrane. *Acta Physiol. Scand.* *109*, 113–114.
- Ammälä, C., Eliasson, L., Bokvist, K., Larsson, O., Ashcroft, F.M., and Rorsman, P. (1993). Exocytosis elicited by action potentials and voltage-clamp calcium currents in individual mouse pancreatic B-cells. *J. Physiol.* *472*, 665–688.
- Barg, S., Huang, P., Eliasson, L., Nelson, D.J., Obermüller, S., Rorsman, P., Thévenod, F., and Renström, E. (2001). Priming of insulin granules for exocytosis by granular Cl⁻ uptake and acidification. *J. Cell Sci.* *114*, 2145–2154.
- Bokvist, K., Holmqvist, M., Gromada, J., and Rorsman, P. (2000). Compound exocytosis in voltage-clamped mouse pancreatic beta-cells revealed by carbon fibre amperometry. *Pflügers Arch.* *439*, 634–645.
- Camacho, M., Machado, J.D., Montesinos, M.S., Criado, M., and Borges, R. (2006). Intragranular pH rapidly modulates exocytosis in adrenal chromaffin cells. *J. Neurochem.* *96*, 324–334.
- Dickerson, L.W., Bonthius, D.J., Schutte, B.C., Yang, B., Barna, T.J., Bailey, M.C., Nehrke, K., Williamson, R.A., and Lamb, F.S. (2002). Altered GABAergic function accompanies hippocampal degeneration in mice lacking ClC-3 voltage-gated chloride channels. *Brain Res.* *958*, 227–250.
- Easom, R.A. (1999). CaM kinase II: a protein kinase with extraordinary talents germane to insulin exocytosis. *Diabetes* *48*, 675–684.
- Easom, R.A., Filler, N.R., Ings, E.M., Tarpley, J., and Landt, M. (1997). Correlation of the activation of Ca²⁺/calmodulin-dependent protein kinase II with the initiation of insulin secretion from perfused pancreatic islets. *Endocrinology* *138*, 2359–2364.
- Eliasson, L., Abdulkader, F., Braun, M., Galvanovskis, J., Hoppa, M.B., and Rorsman, P. (2008). Novel aspects of the molecular mechanisms controlling insulin secretion. *J. Physiol.* *586*, 3313–3324.
- Furuta, M., Carroll, R., Martin, S., Swift, H.H., Ravazzola, M., Orci, L., and Steiner, D.F. (1998). Incomplete processing of proinsulin to insulin accompanied by elevation of Des-31,32 proinsulin intermediates in islets of mice lacking active PC2. *J. Biol. Chem.* *273*, 3431–3437.
- Göpel, S., Zhang, Q., Eliasson, L., Ma, X.S., Galvanovskis, J., Kanno, T., Salehi, A., and Rorsman, P. (2004). Capacitance measurements of exocytosis in mouse pancreatic alpha-, beta- and delta-cells within intact islets of Langenhans. *J. Physiol.* *556*, 711–726.
- Gromada, J., Høy, M., Renström, E., Bokvist, K., Eliasson, L., Göpel, S., and Rorsman, P. (1999). CaM kinase II-dependent mobilization of secretory granules underlies acetylcholine-induced stimulation of exocytosis in mouse pancreatic B-cells. *J. Physiol.* *518*, 745–759.
- Hara-Chikuma, M., Yang, B., Sonawane, N.D., Sasaki, S., Uchida, S., and Verkman, A.S. (2005). ClC-3 chloride channels facilitate endosomal acidification and chloride accumulation. *J. Biol. Chem.* *280*, 1241–1247.
- Høy, M., Olsen, H.L., Bokvist, K., Buschard, K., Barg, S., Rorsman, P., and Gromada, J. (2000). Tolbutamide stimulates exocytosis of glucagon by inhibition of a mitochondrial-like ATP-sensitive K⁺ (KATP) conductance in rat pancreatic A-cells. *J. Physiol.* *527*, 109–120.
- Huang, P., Liu, J., Di, A., Robinson, N.C., Musch, M.W., Kaetzel, M.A., and Nelson, D.J. (2001). Regulation of human CLC-3 channels by multifunctional Ca²⁺/calmodulin-dependent protein kinase. *J. Biol. Chem.* *276*, 20093–20100.
- Hutton, J.C. (1982). The internal pH and membrane potential of the insulin-secretory granule. *Biochem. J.* *204*, 171–178.
- Jentsch, T.J., Stein, V., Weinreich, F., and Zdebik, A.A. (2002). Molecular structure and physiological function of chloride channels. *Physiol. Rev.* *82*, 503–568.
- Kanno, T., Ma, X., Barg, S., Eliasson, L., Galvanovskis, J., Göpel, S., Larsson, M., Renström, E., and Rorsman, P. (2004). Large dense-core vesicle exocytosis in pancreatic beta-cells monitored by capacitance measurements. *Methods* *33*, 302–311.
- Kinard, T.A., Goforth, P.B., Tao, Q., Abood, M.E., Teague, J., and Satin, L.S. (2001). Chloride channels regulate HIT cell volume but cannot fully account for swelling-induced insulin secretion. *Diabetes* *50*, 992–1003.
- Krueger, K.A., Bhatt, H., Landt, M., and Easom, R.A. (1997). Calcium-stimulated phosphorylation of MAP-2 in pancreatic betaTC3-cells is mediated by Ca²⁺/calmodulin-dependent kinase II. *J. Biol. Chem.* *272*, 27464–27469.
- Maritzen, T., Keating, D.J., Neagoe, I., Zdebik, A.A., and Jentsch, T.J. (2008). Role of the vesicular chloride transporter ClC-3 in neuroendocrine tissue. *J. Neurosci.* *28*, 10587–10598.
- Mitchell, J., Wang, X., Zhang, G., Gentsch, M., Nelson, D.J., and Shears, S.B. (2008). An expanded biological repertoire for Ins(3,4,5,6)P4 through its modulation of ClC-3 function. *Curr. Biol.* *18*, 1600–1605.
- Orci, L., Ravazzola, M., Amherdt, M., Madsen, O., Perrelet, A., Vassalli, J.D., and Anderson, R.G. (1986). Conversion of proinsulin to insulin occurs coordinately with acidification of maturing secretory vesicles. *J. Cell Biol.* *103*, 2273–2281.
- Pace, C.S., and Sachs, G. (1982). Glucose-induced proton uptake in secretory granules of beta-cells in monolayer culture. *Am. J. Physiol.* *242*, C382–C387.
- Pothos, E.N., Mosharov, E., Liu, K.P., Setlik, W., Haburcak, M., Baldini, G., Gershon, M.D., Tamir, H., and Sulzer, D. (2002). Stimulation-dependent regulation of the pH, volume and quantal size of bovine and rodent secretory vesicles. *J. Physiol.* *542*, 453–476.
- Robinson, N.C., Huang, P., Kaetzel, M.A., Lamb, F.S., and Nelson, D.J. (2004). Identification of an N-terminal amino acid of the CLC-3 chloride channel critical in phosphorylation-dependent activation of a CaMKII-activated chloride current. *J. Physiol.* *556*, 353–368.
- Rorsman, P., and Renström, E. (2003). Insulin granule dynamics in pancreatic beta cells. *Diabetologia* *46*, 1029–1045.
- Rouillé, Y., Duguay, S.J., Lund, K., Furuta, M., Gong, Q., Lipkind, G., Oliva, A.A., Jr., Chan, S.J., and Steiner, D.F. (1995). Proteolytic processing mechanisms in the biosynthesis of neuroendocrine peptides: the subtilisin-like pro-protein convertases. *Front. Neuroendocrinol.* *16*, 322–361.
- Stiernet, P., Guiot, Y., Gilon, P., and Henquin, J.C. (2006). Glucose acutely decreases pH of secretory granules in mouse pancreatic islets. Mechanisms and influence on insulin secretion. *J. Biol. Chem.* *281*, 22142–22151.
- Stobrawa, S.M., Breiderhoff, T., Takamori, S., Engel, D., Schweizer, M., Zdebik, A.A., Bösl, M.R., Ruether, K., Jahn, H., Draguhn, A., et al. (2001). Disruption of ClC-3, a chloride channel expressed on synaptic vesicles, leads to a loss of the hippocampus. *Neuron* *29*, 185–196.

Thomas, F., Pittman, K., McFadden, T., Haisch, C., Peterson, R., and Thomas, J. (1993). Reversal of type II diabetes by pancreas islet transplant in four separate animal models of type II diabetes. *Transplant. Proc.* 25, 992–993.

Wang, X.Q., Deriy, L.V., Foss, S., Huang, P., Lamb, F.S., Kaetzel, M.A., Bindokas, V., Marks, J.D., and Nelson, D.J. (2006). CLC-3 channels modulate excitatory synaptic transmission in hippocampal neurons. *Neuron* 52, 321–333.

Yoshikawa, M., Uchida, S., Ezaki, J., Rai, T., Hayama, A., Kobayashi, K., Kida, Y., Noda, M., Koike, M., Uchiyama, Y., et al. (2002). CLC-3 deficiency leads to

phenotypes similar to human neuronal ceroid lipofuscinosis. *Genes Cells* 7, 597–605.

Zhu, X., Orci, L., Carroll, R., Norrbom, C., Ravazzola, M., and Steiner, D.F. (2002). Severe block in processing of proinsulin to insulin accompanied by elevation of des-64,65 proinsulin intermediates in islets of mice lacking prohormone convertase 1/3. *Proc. Natl. Acad. Sci. USA* 99, 10299–10304.

Zoccarato, F., Cavallini, L., and Alexandre, A. (1999). The pH-sensitive dye acridine orange as a tool to monitor exocytosis/endocytosis in synaptosomes. *J. Neurochem.* 72, 625–633.